Nonlinear Self-Sustained Drift-Wave Turbulence

J. F. Drake, A. Zeiler, and D. Biskamp
Max-Planck-Institut für Plasmaphysik, D-85748 Garching, Germany
(Received 7 March 1995)

Numerical simulations of 3D collisional drift-wave turbulence in a sheared magnetic field are presented which demonstrate that fluctuations are self-sustaining even though the linear eigenmodes of the system are all damped. An analytic calculation reveals that the source of the turbulence is a nonlinear streaming instability in which radial flows extract energy from the ambient density gradient and drive drift waves which then amplify the radial flow.

PACS numbers: 52.35.Ra, 52.35.Qz, 52.55.Fa

Energy confinement in tokamaks and other plasma fusion experiments is always lower than can be explained by transport by classical interparticle collisions. The source of the anomalous transport has been attributed to measured fluctuations in the density and potential. Drift waves and, in particular, the so-called universal mode were for many years believed to be the source of these fluctuations and transport. This idea was, however, discounted after it was shown that magnetic shear completely stabilizes the universal mode [1] and its collisional counterpart [2]. Later it was shown that magnetic curvature could destabilize drift waves in a toroidal plasma [3]. On the other hand, there has never been any proof that a nonlinear system of equations describing drift-wave turbulence in a sheared magnetic field could not sustain turbulence. Indeed, 2D simulations [4,5] indicated that drift-wave turbulence could be nonlinearly self-sustaining. In neither case was the nature of the nonlinear drive mechanism clear. That the nonlinear behavior of a 3D drift-wave system differs greatly from the 2D case was recently demonstrated by Biskamp and Zeiler [6] who showed that nonlinearly driven convective cells ($\mathbf{B}\cdot\nabla = 0$) were responsible for extracting energy from plasma confined by a straight, nonsheared magnetic field. In the unsheared case collisional drift waves are always unstable so the question of nonlinearly sustained turbulence in a 3D linearly stable system was not addressed. In this paper we present 3D simulations of drift-wave turbulence in a sheared magnetic field which demonstrate the persistence of turbulence even in the absence of linear instability. We also present a simple picture of the nature of the nonlinear drive mechanism which is supported by analytic calculations and simulations.

In a magnetic field aligned coordinate system, in which z lies along $\mathbf{B}$, the ambient density gradient is in the x direction and the y direction is defined by $\mathbf{B}\cdot\nabla y = 0$, the coupled equations for perturbations of the density n, potential φ, and parallel flow v_z in a straight sheared magnetic field are given by

$$\frac{dn}{dt} + \frac{\partial\varphi}{\partial y} + \hat{\rho}^2\frac{\partial^2}{\partial z^2}(\varphi - n) + \gamma\frac{\partial v_z}{\partial z} = 0, \quad (1)$$

$$\frac{d}{dt}\nabla_\perp^2\varphi + \frac{\partial^2}{\partial z^2}(\varphi - n) = 0, \quad (2)$$

$$\frac{dv_z}{dt} + \gamma\frac{\partial n}{\partial z} = 0, \quad (3)$$

where $T_i = 0$, T_e is assumed to be a constant, and

$$\nabla_\perp^2 = \left(\frac{\partial}{\partial x} + z\frac{\partial}{\partial y}\right)^2 + \frac{\partial^2}{\partial y^2},$$

$$\frac{d}{dt} = \frac{\partial}{\partial t} + \hat{z}\times\nabla\varphi\cdot\nabla, \quad (4)$$

with $\hat{\rho} = \rho_s/L_\perp$ and $\gamma = c_s t_d/L_s$. The equations have been normalized using the magnetic shear length L_s as the parallel scale length, the perpendicular length $L_\perp = (\nu_e L_s^2\rho_s^2/\Omega_e L_n)^{1/3}$, and the diamagnetic time scale $t_d = L_n L_\perp/\rho_s c_s$. In the absence of magnetic shear the term proportional to z in (4) is absent. In these normalized units $n/n_0 \sim e\varphi/T_e \sim v_z/c_s \sim L_\perp/L_n$ and the transport scales like

$$D_\perp \sim L_\perp^2/t_d \sim \rho_s c_s L_\perp/L_n. \quad (5)$$

Small diffusive dissipation terms are added to each equation to model ion viscosity and classical transport. The ambient density gradient which has been absorbed into the normalization of the variables enters the equations through the $\partial\phi/\partial y$ term in (1). The energy equation constructed from (1)–(3) yields

$$\frac{1}{2}\frac{\partial}{\partial t}\int dx^3(\hat{\rho}^2|\nabla_\perp\varphi|^2 + n^2 + v_z^2) = -\hat{\rho}^2\int dx^3\left(\frac{\partial\varphi}{\partial z} - \frac{\partial n}{\partial z}\right)^2 - \int dx^3\, n\frac{\partial\varphi}{\partial y}, \quad (6)$$

where the perpendicular dissipation terms are ignored. While the parallel dissipation term on the right side of the equation is negative, the remaining term, which arises from the ambient density gradient, has no definite sign. Thus nonlinear instability is not precluded.

In the simulations (1), (2), and (3) are stepped in time with the $\partial^2/\partial z^2$ operators approximated with a second order finite difference scheme and advanced implicitly. Periodic boundary conditions are imposed in the transverse directions with convection terms treated either with a fourth-order, finite difference, or a pseudospectral scheme. In the z direction the system is split into modules of length 2π. This is necessary because the flux tube coordinate system becomes increasingly distorted with respect to the

 0031-9007/95/75(23)/4222(4)$06.00

physical system as z becomes large and structures in the physical system can no longer be correctly resolved. The solutions at the z boundaries of each module are mapped to the adjacent module by untwisting them and retwisting them to match the adjacent module. The grid consists of up to $128 \times 128 \times 90$ cells.

If the simulations are initialized by applying small, random perturbations of n and φ, the fluctuations die away since there is no linear instability. To facilitate the growth of the turbulence to finite amplitude, we include magnetic curvature in Eqs. (1) and (2) [7,8], which gives rise to linear drift-ballooning instability similar to the Raleigh-Taylor instability of a system with a gravitational field acting on a neutral fluid. Shown in Fig. 1 is the total energy versus time from a simulation with $L_x = 9.8$, $L_y = 10.2$, $L_z = 18.9$, and $\hat{\rho} = 0.79$. The parameters correspond to a regime where the diamagnetic frequency exceeds the local interchange growth rate and the ballooning effect is weak. At $t = 666$ we turned off the magnetic curvature, so that the equations reduced to (1)–(3) above, making the system linearly stable. Nevertheless, the turbulence remains at a quasisteady finite level. Figure 2 shows a typical density perturbation in the x-y plane from the same simulation. The important question is why the nonlinear equations produce finite fluctuations and transport even though all modes are linearly stable. A clue comes from the occasional appearance of regions of intense transport, where radially extended flows v_x form, strengthen, and then break up. We show now that the turbulence results from the nonlinear amplification of these x-directed flows. Figure 3 illustrates the physical mechanism. The flow $v_x(y)$ convects the ambient density up and down the density gradient and therefore produces the density perturbation $n_0(y)$, Fig. 3(a). When this density perturbation becomes sufficiently large, it destabilizes drift waves with $k_x > k_y$ and finite k_z. These drift waves are not stabilized by magnetic shear because their wave vector is essentially oriented in the z-x plane and the magnetic shear acts primarily on disturbances with large k_y. The growing potential perturbation of this drift wave is shown in Fig. 3(b). The potential perturbations of the drift-wave amplify the original x-directed flows shown in Fig. 3(a). The mechanism shown in Fig. 3(c) is basically the vortex peeling process presented previously for the self-generation of sheared poloidal rotation [9]. Thus the entire process is self-amplifying and is apparently insensitive to the magnetic shear.

To estimate the growth of this streaming instability we present a simple analytical model which describes the nonlinear interaction of a truncated set of modes. For simplicity, the calculation is carried out in an unsheared system, although magnetic shear should not alter the qualitative picture. Previous investigations of sheared flow generation focused on how stable vortices [9] or drift waves [10] interacted to drive sheared flow. We extend this approach by allowing the drift waves to be self-consistently amplified by self-generated gradients. The flows are described by three interacting potential perturbations

$$\phi = \phi_0 \cos(\pi y) + (\phi_1 \cos \pi y + \phi_2 \sin 2\pi y) \times \sin k_z z \exp(i k_x x), \quad (7)$$

where ϕ_0 describes the radial sheared flow and ϕ_1 and ϕ_2 are drift waves whose phase in y has been chosen so that they interact to drive ϕ_0. The mode ϕ_2, which has a shorter wavelength, is taken to be damped by perpendicular viscosity. We take $k_x \gg k_y \sim 1$ so that the two drift waves essentially propagate along x due to the density gradient $\partial n/\partial y$ as shown in Fig. 3, i.e., the configuration is rotated by $\pi/2$ compared with a conventional drift wave. At the same time the sheared flow which is generated is radial rather than poloidal, and this flow drives the nonlinear instability. The corresponding density perturbations are similar to those of ϕ with the exception of $n_0(y)$, which is driven by the radial convection $(\partial \phi_0/\partial y)$ of the initial ambient density gradient. The drift waves

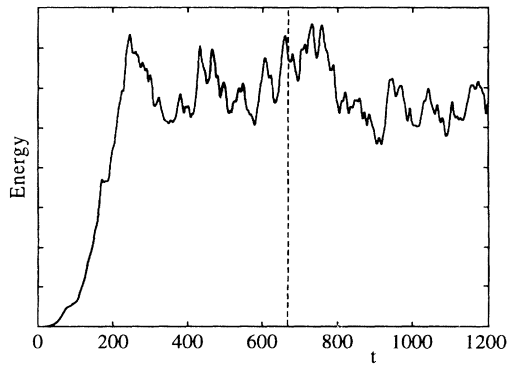

FIG. 1. The total energy versus time from a simulation with magnetic shear including magnetic curvature for $t < 666$.

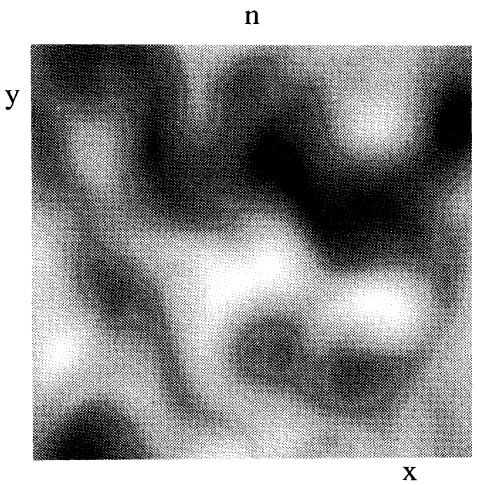

FIG. 2. A grey scale plot of n perpendicular to **B** with light shading corresponding to high density.

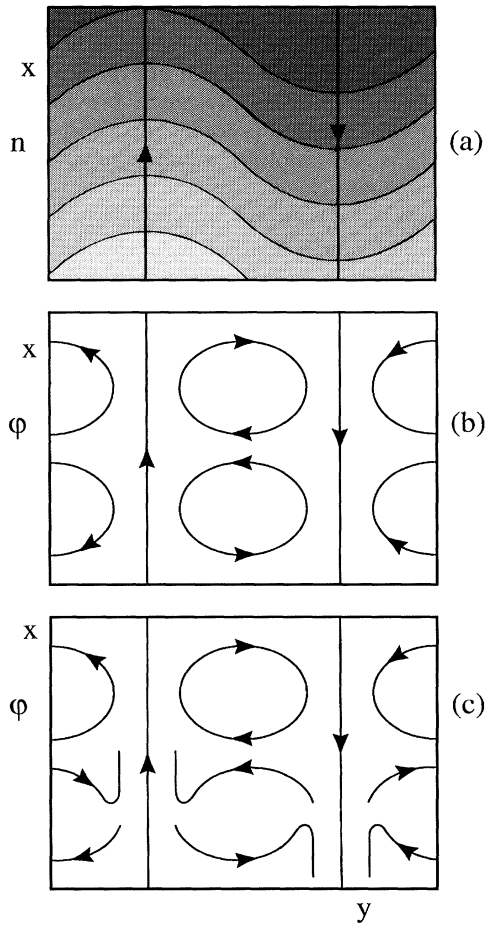

FIG. 3. Physical mechanism of the nonlinear instability.

growing on the local gradient $n_{0y} \equiv \partial n_0/\partial y$ grow most strongly on the steepest part of the gradient. The resulting quasilinear flattening of the density profile evens the gradient, forcing $n_0(y)$ to take on a triangular shape with n_{0y} being piecewise constant, i.e., n_{0y} is a positive (negative) constant between (outside) the vertical flow lines in Fig. 3(a). To evaluate the time dependence of n_{0y} we take the y derivative of (1) and average over z, x, and the y interval $(-1/2, 1/2)$, which yields

$$\partial n_{0y}/\partial t = 2\pi\phi_0 , \tag{8}$$

with n_{0y} a piecewise constant. Note that the average eliminates both the convective transport and compression terms in (1). The remaining interactions between the modes can be evaluated without further approximation. The final equations are

$$\partial\phi_1/\partial t + \gamma_1(\phi_1 - n_1) + A_{1\phi}\phi_0^2\phi_1 = 0 , \tag{9}$$

$$\partial n_1/\partial t + \gamma_1 k_{\perp 1}^2\hat{\rho}^2(n_1 - \phi_1) + A_{1n}\phi_0^2 n_1 - ik_x n_{0y}\phi_1 = 0 , \tag{10}$$

$$\partial\phi_0/\partial t = A_0|\phi_1|^2\phi_0 , \tag{11}$$

where $\gamma_1 = k_z^2/k_{\perp 1}^2$, $k_{\perp i}^2 = k_{xi}^2 + k_{yi}^2$, $A_0 = k_x^2(k_{\perp 2}^2 - k_{\perp 1}^2)(k_{\perp 1}^2 - k_{\perp 0}^2)8k_{\perp 2}^2\nu_{2\phi}$, $A_{1\phi} = A_0 2\pi^2/k_{\perp 1}^2$, $A_{1n} = k_x^2\pi^2/4\nu_{2n}$, and ν_{2n} and $\nu_{2\phi}$ are the damping rates of n_2 and ϕ_2. In the absence of radial flow, (9) and (10) are linear, yielding the local dispersion relation for the complex growth rate γ,

$$\gamma\left(1 + k_{\perp 1}^2\hat{\rho}^2 + \gamma\frac{k_{\perp 1}^2}{k_z^2}\right) = -ik_x n_{0y} , \tag{12}$$

of drift waves driven unstable by n_{0y}. An initial small radial flow ϕ_0 increases n_{0y} in (8). The drift waves described by (9) and (10) go unstable, amplifying ϕ_0 in (11), which then further increases n_{0y}. As ϕ_0 grows, the shear flow damping terms in (9) and (10), proportional to ϕ_0^2, become important and the system evolves in such a way that the drift waves remain near marginal stability, the drive due to n_{0y} balancing the damping due to ϕ_0. The balance gives (assuming $\mathrm{Re}\gamma = 0$)

$$\phi_0^4 = \frac{k_x n_{0y}\gamma_1}{(A_{1\phi} + A_{1n})(A_{1n}A_{1\phi})^{1/2}} \equiv \hat{\gamma}_1 n_{0y} . \tag{13}$$

Inserting this result into (8) yields a nonlinear evolution equation for n_{0y},

$$\partial n_{0y}/\partial t = 2\pi\hat{\gamma}_1^{1/4} n_{0y}^{1/4} , \tag{14}$$

with the algebraically growing solution $n_{0y} \sim t^{4/3}$.

To test this picture of nonlinear instability, we have performed 3D simulations of drift-wave turbulence in the case of no magnetic shear. The system is initialized with $n_0(y)$ of the lowest order mode of the system of sufficiently large amplitude to locally drive drift-wave turbulence. The parameters of the simulation are $L_x = 18$, $L_y = 36$, $L_z = 72$, and $\hat{\rho} = 1.0$. In the nonlinear instability the extraction of energy from the ambient gradient arises from the $k_z = 0$ component of v_x in contrast with the usual linear drift-wave theory where k_z is finite. To focus on the nonlinear instability, we artificially eliminate $k_z \neq 0$ components of the $\partial\varphi/\partial y$ drive term in the continuity equation, which makes the system linearly stable. In Fig. 4 time traces of the energy in all modes (thick solid), $k_z = 0$ modes (short-dashed), and $k_z \neq 0$ modes (long-dashed) are shown. At around $t = 25$ the modes with $k_z \neq 0$ (drift waves) grow strongly at the expense of $k_z = 0[n_0(y)]$. After this initial transient, all of the energies begin to grow steadily with no apparent saturation. A 2D slice of the potential during this later phase is shown in Fig. 5. The large scale radial flow $v_{x0}(y)$ dominates. This flow has been amplified from noise. Time sequences of such plots (not shown) reveal that the peeling of the drift-wave vortices is the dominant mechanism for amplifying the radial flow at late time. The corresponding 2D plots of the density are similar and reveal that $n_0(y)$ has also been amplified during the simulation. Finally, the thin solid curve in Fig. 4 is the time history of the energy with the usual linear drift-wave drive included. The qualitative features are similar. Thus

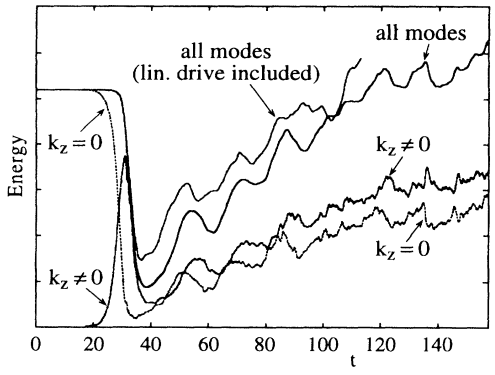

FIG. 4. Energy versus time from a simulation with no magnetic shear.

the usual linear drift-wave instability plays no significant role in the nonlinear evolution of the system.

The next issue is whether the nonlinear instability just described underlies the dynamics of sustained turbulence observed in the presence of magnetic shear. At the qualitative level, regions where the transport occasionally becomes very large exhibit radially extended flows. The analytic calculation is almost unchanged when magnetic shear is included. There is no exact $k_z = 0$ mode in a sheared magnetic field. A radial flow at some location along the flux tube in a sheared magnetic field twists in the x-y plane and is compressed in the x direction as it projects down the flux tube [11]. As a consequence, radial flows are localized in the z direction and develop a finite k_z and the associated damping which must be overcome by the nonlinear drive. A crucial test of the physical picture of the nonlinear instability mechanism

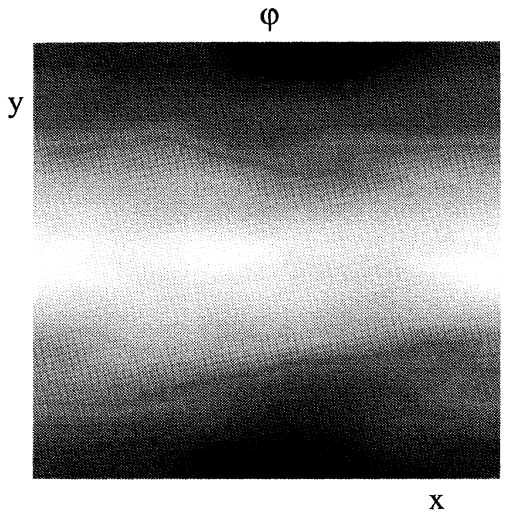

FIG. 5. A grey scale of ϕ perpendicular to **B** illustrating the development of the radial flow.

is that the source of energy of density fluctuations is $k_z \sim 0$ modes rather than finite k_z modes as would be expected from a traditional linear drift wave model. A spectral analysis of Eq. (1) as carried out in Ref. [6] reveals that the source of energy is indeed the longest wavelength (small k_z) density disturbances in the system. The primary reason that the nonlinear instability remains robust in a sheared magnetic field is that the drift waves driven by $n_0(y)$ are not stabilized by magnetic shear because these modes have $k_x \gg k_y$ and k_x is not affected by magnetic shear, i.e., magnetic shear drops out of (1) and (2) if $k_y = 0$. The fundamental difference between a sheared and nonsheared system is therefore not the mechanism which drives the turbulence but the saturation mechanism. In the unsheared magnetic field the energy runs away as the radial flows continue to amplify, while in a sheared system the radial flows always break up as a result of Kelvin-Helmholtz instability, leading to a saturated nonlinear state.

In conclusion, we have found that the drift-wave turbulence in a plasma confined by a magnetic field is driven by a nonlinear streaming instability. This instability is essentially independent of the magnetic shear. While the present results are based on a collisional description of drift waves, the basic mechanism for the nonlinear instability presented in Fig. 3 does not depend on the collisionality of the system. Collisionless drift waves would grow on the density gradient n_{0y} and then reinforce the radial sheared flow. Thus it seems possible that the core confinement region of a tokamak would also be subject to nonlinear instability, and this mechanism would compete with trapped particle instabilities in driving transport.

J. F. D. acknowledges the support of the Humboldt Foundation through a Senior Scientist Research Award. We would like to thank Dr. Bruce Scott for significant discussions on the nature of drift-wave turbulence and Dr. Parvez Guzdar for discussions on the generation of poloidal sheared flow.

[1] T. M. Antonsen, Phys. Rev. Lett. **41**, 33 (1978).
[2] P. N. Guzdar, L. Chen, P. K. Kaw, and C. Oberman, Phys. Rev. Lett. **40**, 1566 (1978).
[3] C. Z. Cheng and L. Chen, Phys. Fluids **23**, 2242 (1989).
[4] D. Biskamp and M. Walter, Phys. Lett. **109A**, 34 (1985).
[5] B. D. Scott, Phys. Rev. Lett. **65**, 3289 (1990).
[6] D. Biskamp and A. Zeiler, Phys. Rev. Lett. **74**, 706 (1995).
[7] P. N. Guzdar *et al.*, Phys. Fluids **B3**, 3712 (1993).
[8] J. F. Drake *et al.*, in *Plasma Physics and Controlled Nuclear Fusion Research* (IAEA, Vienna, 1994), paper D-P-I-8.
[9] J. F. Drake *et al.*, Phys. Fluids **B4**, 488 (1992).
[10] P. N. Guzdar (to be published).
[11] K. V. Roberts and J. B. Taylor, Phys. Fluids **8**, 315 (1965).

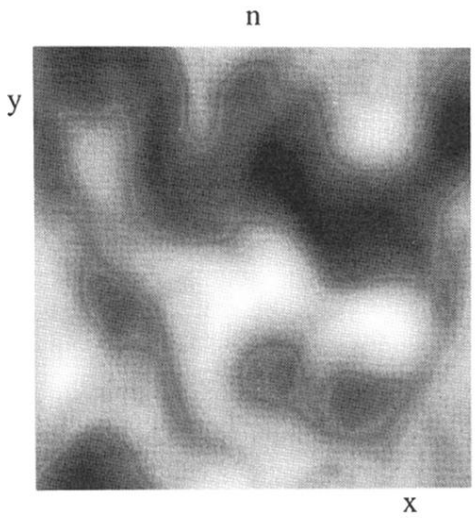

FIG. 2. A grey scale plot of n perpendicular to **B** with light shading corresponding to high density.

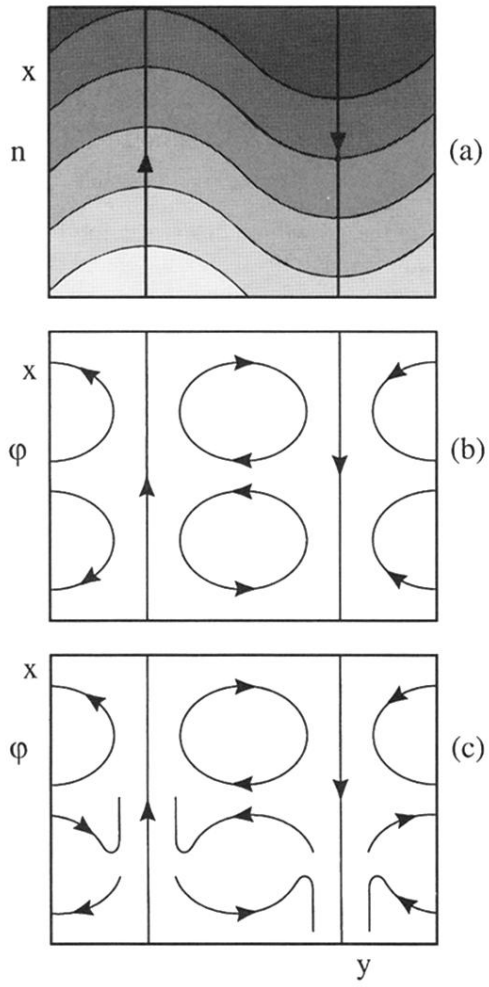

FIG. 3. Physical mechanism of the nonlinear instability.

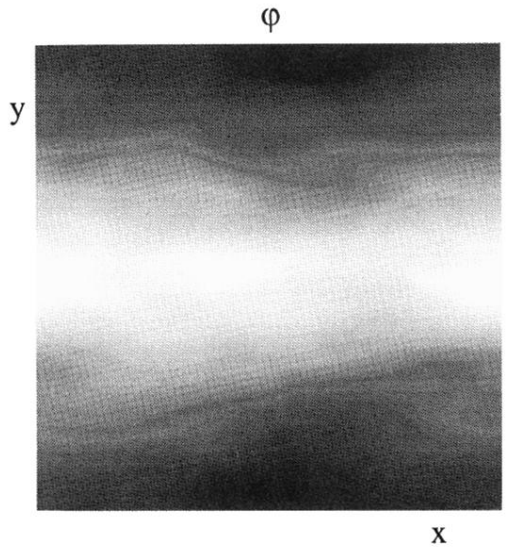

FIG. 5. A grey scale of ϕ perpendicular to **B** illustrating the development of the radial flow.